Moho Depth along the Antarctic Peninsula and Crustal Structure across the Landward Projection of the Hero Fracture Zone

Tomasz Janik[1*] · Piotr Środa[1] · Marek Grad[2] · Aleksander Guterch[1]

[1]Institute of Geophysics, Polish Academy of Sciences, Ks.Janusza 64, 01-452 Warsaw, Poland , *<janik@igf.edu.pl>
[2]Institute of Geophysics, University of Warsaw, Pasteura 7, 02-093 Warsaw, Poland

Abstract. Results of deep seismic soundings collected during four Polish Geodynamical Expeditions to West Antarctica between 1979 and 1991 have been synthesised to produce a map of Moho depth beneath the NW coast of the Antarctic Peninsula. In this paper, we present a new interpretation of the deep landward projection of the Hero Fracture Zone based on two seismic transects. On each transect we found high velocity bodies with Vp>7.2 km s^{-1}, similar to ones we detected previously in Bransfield Strait. However, these bodies are not continuous; they are separated by a zone of lower velocities located SW of Deception Island. In Bransfield Strait an asymmetric "mushroom"-shaped high velocity body was found at a depth interval from 13-18 km down to the Moho boundary at a depth of ca. 30 km. As a summary of results, we present a map of Moho depth along the coast of the Antarctic Peninsula, prepared using previous seismic 2-D models. The maps shows variations in crustal thickness from 38-42 km along the Antarctic Peninsula shelf in the southern part of the study area to 12-18 km beneath the South Shetland Trench.

Introduction

During four Polish Antarctic geodynamical expeditions between 1979 and 1991, deep seismic sounding (DSS) measurements were performed in the transition zone between the Drake and South Shetland microplates and the Antarctic plate in West Antarctica. The network of 20 DSS profiles ranging in length from 150 to 320 km covered the western side of the Antarctic Peninsula from Adelaide Island in the south to Elephant Island on the north (Fig. 5.2-1). The seismic results obtained during four expeditions, were published in a number of papers (Guterch et al. 1985, 1991, 1998; Grad et al. 1992, 1993, 1997, 2002; Janik 1997a,b; Środa et al., 1997; Środa, 2001, 2002). This paper presents new 2-D seismic models for a network of six jointly modelled profiles along two seismic transects: Transect I - DSS-10, DSS-7 and DSS-2 (together 660 km long); Transect II - DSS-6, DSS-15 and DSS-5 (460 km). Both transects were sub-parallel to the northwestern coast of the Antarctic Peninsula, crossing the transition zone from a passive to an active margin and main structures of the Bransfield Strait (Fig. 5.2-1). Based on these results and previous models, a map of Moho depth along western coast of the Antarctic Peninsula was prepared.

Tectonic Setting

The tectonic history of the western margin of the Antarctic Peninsula has been reconstructed mainly from surface distribution of marine magnetic anomalies on the neighbouring sea floor by many authors (e.g., Herron and Tucholke 1976, Barker 1982). Ocean crust formed at the Aluk Ridge (Fig. 5.2-1) must have been subducted beneath the peninsula, until segments of the ridge itself arrived at the margin and subduction stopped. Subduction and spreading stopped along well defined segments of the margin at different times, the spreading ridge topography disappeared and the zone where the ridge segment had arrived became a passive margin. These processes repeated in successive segments of the subducting plate, separated by numerous fracture zones. According to Larter and Barker (1991), this process occurred until about 5.5-3.1 million years ago when the last segment of the ridge reached the section of the margin south of the Hero Fracture Zone (HFZ). The date of last ridge segment arrival at margin becomes 6.4-3.3 Ma when the Cande and Kent (1995) magnetic reversal timescale (MRTS) is used (Larter et al. 1997). Between the latter and the Shackleton Fracture Zone (SFZ), there is the last preserved, although now inactive, fragment of the Aluk-Antarctic spreading axis. Spreading has now stopped on this ridge (Larter and Barker 1991; Livemore et al. 2000; Eagles 2004).

The landward projection of HFZ separates the South Shetland Islands and the Bransfield Basin from a continental, passive zone further to the south (Herron and Tucholke 1976). Several tectonic lineaments, discontinuities and geological structures between Deception and Low islands were presented in many papers and interpreted as landward projections of HFZ. Interpretation of detailed long-range sidescan sonar data and multichannel seismic reflection profiles shows that the South Shetland Trench continues 50 km southwest of the HFZ (Tomlinson at al. 1992; Maldonado at al. 1994; Jabaloy et al. 2003). Henriet et al. (1992) presented ~50 km wide HFZ and Smith Island, a blueschist terrane showing evidence of considerable uplift, located exactly in front of the HFZ. They interpreted a trough southwest of HFZ as a fossil rift valley of the Aluk Ridge and suggested

From: Fütterer DK, Damaske D, Kleinschmidt G, Miller H, Tessensohn F (eds) (2006) Antarctica: Contributions to global earth sciences. Springer-Verlag, Berlin Heidelberg New York, pp 229-236

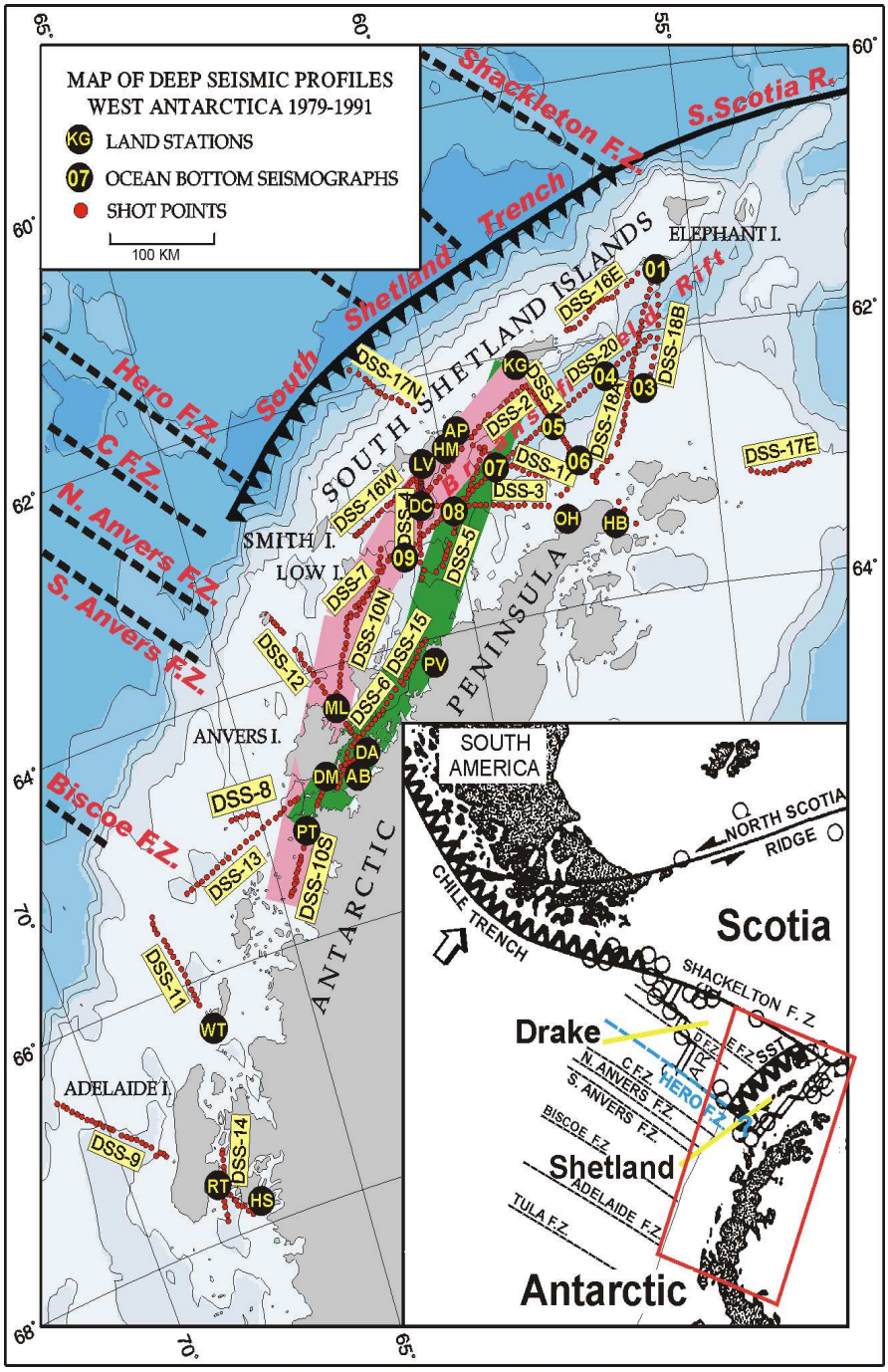

Fig. 5.2-1. Location of deep seismic soundings (DSS) profiles and transects in West Antarctica. *Seismic* stations: *AB:* Almirante Brown, *AP:* Arturo Prat, *DA:* Danco, *DC:* at Deception Island, *DM:* Damoy, *HB:* Hope Bay, *HM:* at Half Moon Island, *HS:* Horse Shoe, *KG:* at King George Island, *LV:* at Livingston Island, *ML:* Melchior, *OH:* O'Higgins, *PT:* Petermann, *PV:* Primavera, *RT:* Rothera, *WT:* Watkins, *01-09:* ocean bottom seismographs. Transect I *(pink stripe):* DSS-10 + DSS-7 + DSS-2; Transect II *(green stripe):* DSS-6 + DSS-15 + DSS-5. The positions of fracture zones *(F.Z.)*, the South Scotia Ridge (S. Scotia R.) are taken from Barker (1982), Larter and Barker (1991) with modifications after Tomlinson et. al (1992). Bathymetry contours are plotted at 500 m intervals (ETOPO5 data file, NOAA's NGDC), using GMT software by Wessel and Smith (1995). Inset: Plate tectonic elements around the Scotia region from Tectonic Map of the Scotia Arc (1985), and Birkenmajer et al. (1990). Abbreviations: *SST:* South Shetland Trench; *AR:* Aluk Ridge: divergent plate boundary, ridge and transform faults; *open arrows* show direction of subduction; *double, black arrows* present relative motion at the North Scotia Ridge plate boundary; *white circles:* epicentres of the 1963-1985 earthquakes (for earthquakes with mb > 5.0) by Pelayo and Wiens (1989); *dashed lines* show fracture zone trends. The *red box* shows the location of the study area.

that spreading stopped some 5 Ma ago, shortly before the ridge collided with the trench. The width and position of the ridge associated with HFZ was clear from bathymetry map published by Larter and Barker (1991), and its orientation was confirmed by interpretation of GLORIA data published by Tomlinson et al. (1992). From this, it is clear that any such fossil rift valley would have been oblique to the margin. In fact the trough described by Henriet et al (1992) is the part of the South Shetland Trench that continues to the south of the HFZ, which is seen very clearly in the GLORIA sidescan sonar data presented by Maldonado et al. (1994). Jabaloy et al. (2003) identified here two active major reverse faults. A seismic reflection profile running along Boyd Strait (Jin et al. 2003), just northwest of the landward projection of the HFZ, shows major structural components similar to those typically observed along the margin to the southwest of the HFZ. The continuation of the post-subduction margin structures to the active margin suggests that the boundary between crust with passive and active margins characteristics is not sharply defined.

Seismic Modelling

Examples of seismic record sections and 2-D modelling are presented on Fig. 5.2-2. The travel times of refracted and reflected P waves, correlated in the record sections

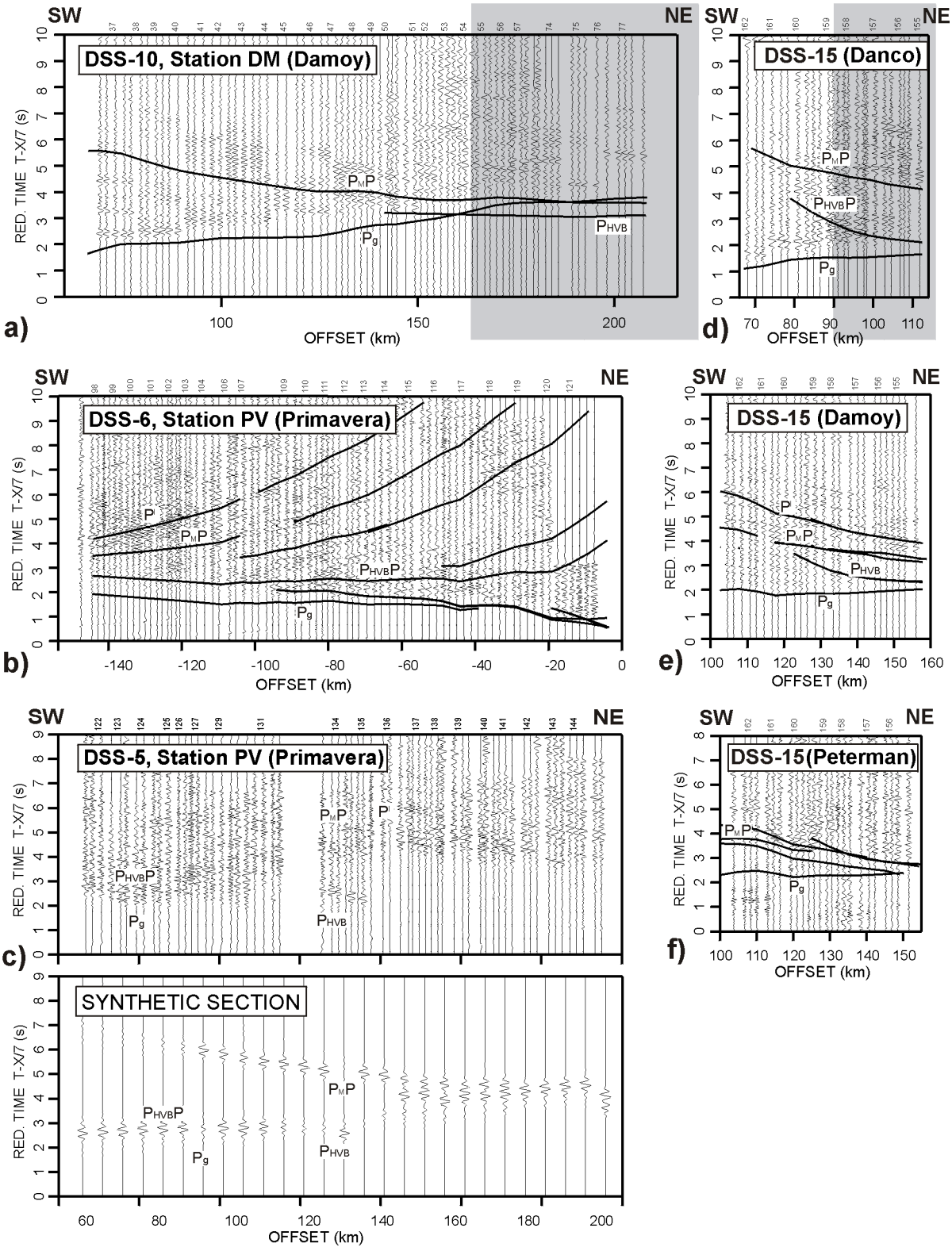

Fig. 5.2-2. Amplitude-normalised seismic record sections and theoretical travel times of P waves calculated for the crustal model for Transect I: **a** *DSS-10 profile, station DM* (Damoy I.); and Transect II: **b** *DSS-6 profile, station PV* (Primavera); **c** *DSS-5 profile, station PV* (Primavera) and for **d** *DSS-15 profile, station DA* (Danco Island), station *DM* (Damoy) **e**, station *PT* (Petermann) **f**. Abbreviations: *Pg*: refracted arrivals from the crust, *PHVB*: waves penetrated HVB, *PHVBP*: reflection from the top of the HVB, *PMP*: reflection from the Moho discontinuity, *P*: lower lithosphere phases. *Bottom diagram* of panel **c** presents synthetic section. Reduction velocity 7.0 km s^{-1}. *Grey shading area* shows range of HVB.

along the profiles, provide the basis for the modelling of the velocity distribution and depths to the seismic boundaries in the seismic models of the crust and uppermost mantle (Fig. 5.2-3). For 2-D modelling of the velocity structure we applied the ray tracing technique for calculations of traveltimes and synthetic seismograms using the interactive version of package SEIS83 (Červený and Pšenčík 1983) supported by graphical interfaces MODEL (Komminaho 1998) and ZPLOT (Zelt 1994). Results of 2-D modelling of the network of linear DSS profiles provide images of the very complicated deep structure of the Earth's crust in the Bransfield Strait and along the margin of the Antarctic Peninsula. Examples of results of the 2-D modelling for different parts of the transects are shown in Fig. 5.2-2.

Crustal Models

The seismic models of the crust and uppermost mantle (Fig. 5.2-3) along both transects cross the transition zone between the passive and active margins of the northwestern coast of the Antarctic Peninsula and the main structures of the Bransfield Strait.

Transect I

A ca. 70 km long, high velocity body (HVB), with $Vp > 7.2$ km s^{-1} was modelled at km 360-430 from 12 km down to the Moho boundary located here at a depth of 35 km. The SW part of the model (DSS-10S) is after Środa et al., (1997). In the upper crust, a layer with velocities 6.3-6.4 km s^{-1} down to 12 km depth was found. In the central and NE parts of the transect, layers with Vp <5.8 km s^{-1} were modelled in the upper crust. This difference is also evident in the lower crust where velocities are 7.1-7.25 km s^{-1} in the southwestern part and 7.25-7.4 km s^{-1} in the northeastern part. The crustal thickness decreases from 36-39 km in the southwest and central parts of the transect to 31 km in the northeastern part. Sub-Moho velocities of 8.05 km s^{-1} and a deep reflector (55-45 km, at distances 210-600 km) were modelled for the upper mantle.

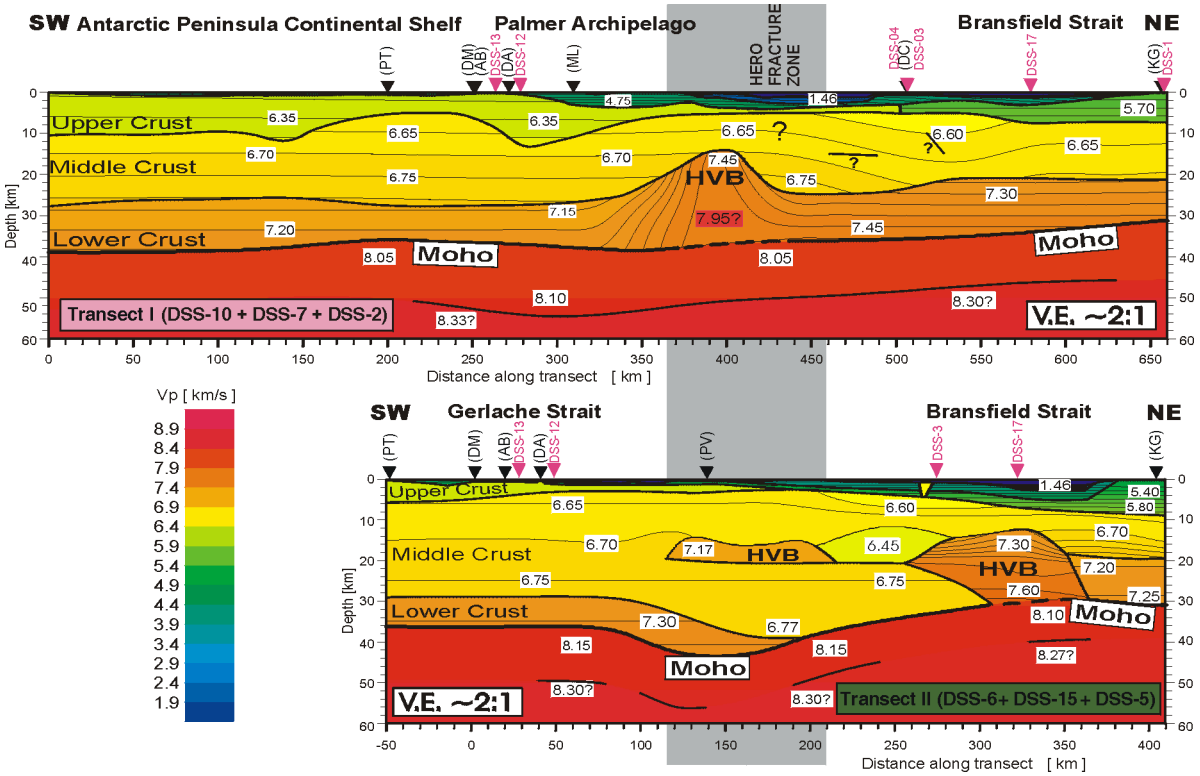

Fig. 5.2-3. Two-dimensional, P-wave velocity models across the contact zone between passive continental margin of the Antarctic Peninsula shelf and the active marginal zone in the area of Bransfield Strait, along two transects between Petermann Island (*PT*) and King George Island: Transect I – profiles: *DSS-10*, *DSS-7* and *DSS-2* (SW part of the model, *DSS-10S*, after Środa et al. (1997); Transect II – profiles: *DSS-6*, *DSS-15* and *DSS-5*. *Thick, black lines* represent major velocity discontinuities (interfaces). *Thin lines* represent velocity isolines with values (km/s) shown in *white boxes*. The *red box* shows velocity of HVB required by data recorded on Melchior (*ML*) station only. *Black arrows* show positions of stations and *red arrows* crossings with other DSS profiles. Other explanations as in Fig. 5.2-1.

Transect II

Two high velocities bodies were modelled; the first, ca. 80 km long and 5 km thick, with $Vp > 7.1$ km s^{-1}, was modelled at km 170 at a depth of 15 km; the second one, in the central part of Bransfield Strait, with Vp = 7.2-7.7 km s^{-1} at km 250-360 extends from a depth of 13 km down to the Moho boundary. The bodies are separated by a low velocity zone with Vp<6.4 km s^{-1}. In the central part of the transect, velocities Vp~6.7 km s^{-1}, typical for middle crust, were modelled down to the Moho boundary which reaches depth of 42 km in this area. The lower crustal velocities are 7.3 km s^{-1} in the 7 km thick southwestern part and 7.2 km s^{-1} in the 12 km thick northeastern part of the model. Sub-Moho velocities 8.10-8.15 km s^{-1} and a deep reflector (55-40 km) at distances 100-400 km were modelled for the upper mantle.

Images of the crustal structure along the transects are different. Along Transect I, located more to the northwest, the HVB (Vp>7.2 km s^{-1}) is very clearly expressed, being about 70 km wide at a depth from 12 km to the Moho boundary. The pattern of HVB on the Transect II, is different, ~100 km wide and only 5 km thick, but the Moho boundary is the deepest beneath HVB (42 km). The existence of a HVB was not confirmed further to the NE. Velocities of a Vp<6.5 km s^{-1} at depths 10-15 km and Vp=6.6-6.75 km s^{-1} at depths 6-20 km were detected on Transects II and I respectively, southwest from the Deception Island. Similar low velocities were detected on DSS-4 at depths 7-15 km (Janik 1997a,b). The seismic results obtained for the Bransfield Strait are summarized in Fig. 5.2-4.

Map of the Moho Depth

Based on the models of crustal structure presented here, as well as on previous results of seismic modelling (Grad et al. 2002; Guterch et al. 1998), a map of isolines of depth to the Moho discontinuity along the Antarctic Peninsula was prepared (Fig. 5). The depth to the Moho values were taken where available along all profiles. Between the data points the Moho depth was interpolated

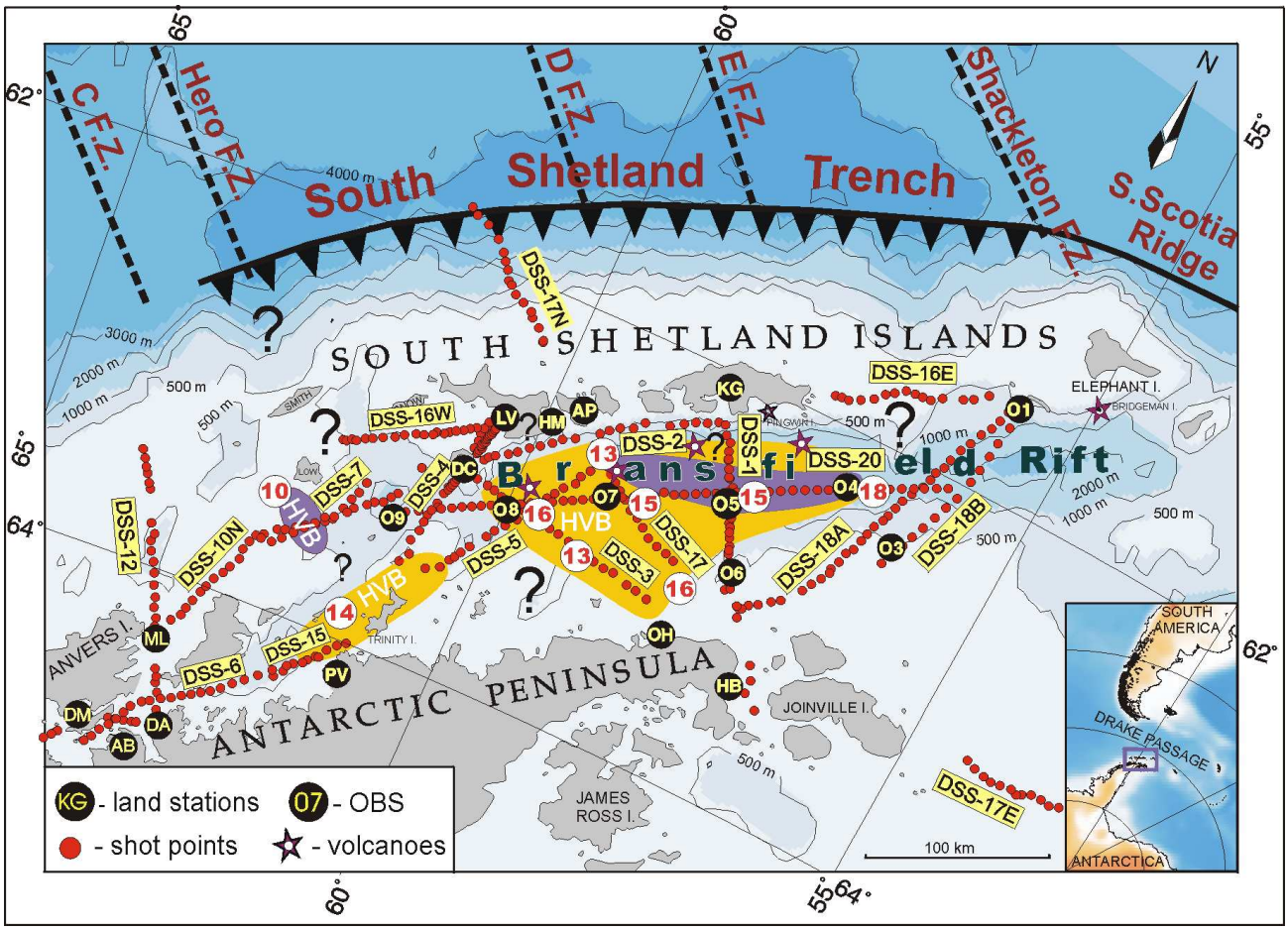

Fig. 5.2-4. P-wave velocity anomalies detected in the crust in the Bransfield Strait marginal basin against of the South Shetland Islands. Range of the previously identified high velocity (mushroom-shaped) body (HVB) with Vp>7.2 km s^{-1} in the Bransfield Strait, detected at a depth of 10-18 km, deduced from two-dimensional modelling of the net of intersecting deep seismic profiles. *Violet colour* shows the places where the depth of high velocity body reaches 30 km. At other places (*yellow colour*), the thickness of the body is relatively small (southern part) or unknown (northwest part).

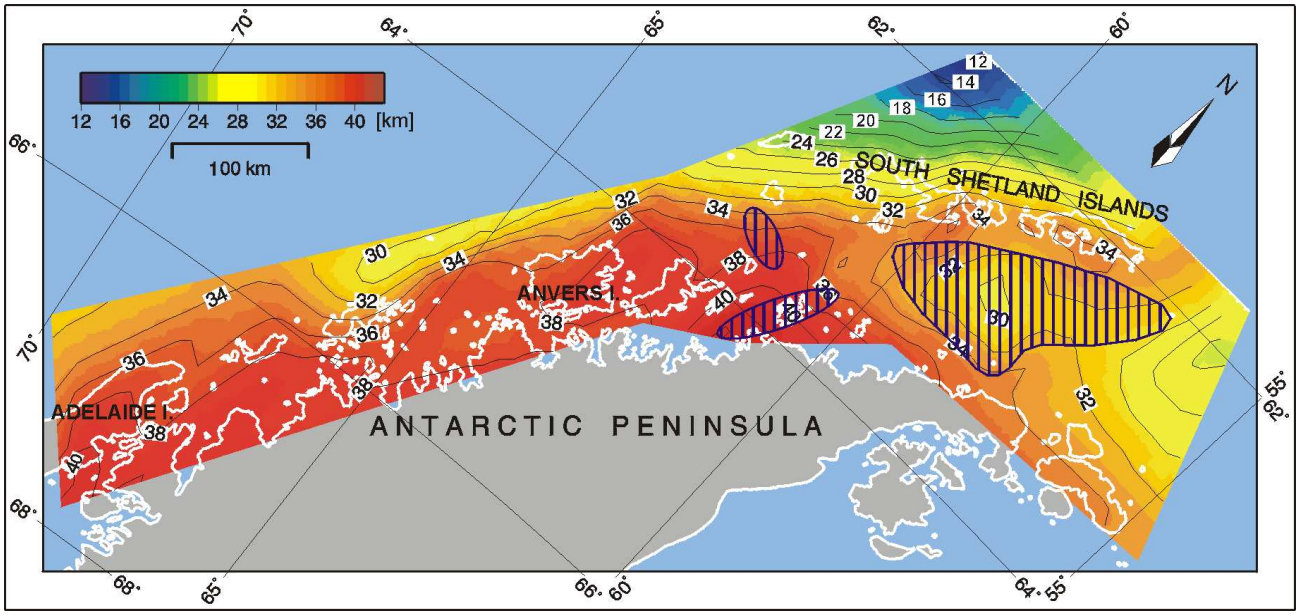

Fig. 5.2-5. Map of the depth to the Moho boundary along the Antarctic Peninsula, based on data from raytracing models of the crustal structure. Areas filled with blue lines in the central part of the Bransfield Strait mark the extent of the high velocity anomaly, where at a depth of 13-18 km P-wave velocities reach 7.2 km s^{-1}, as well as the extent of two other areas of anomalously high velocity. In the NE part of this area, due to possible existence of a thick crust-mantle transition, the isolines do not reflect the actual Moho depth (see Fig. 5.2-4).

to create a 2-D surface. The map shows that the maximum crustal thickness, 38-42 km, occurs along the Antarctic Peninsula shelf between Adelaide Island and Palmer archipelago. Towards the Pacific, the Moho depth decreases and reaches 30-32 km at the edge of study area. In central part of the Bransfield Strait, seismic velocities reach anomalously high value of 7.2 km s^{-1} at a body that is asymmetric "mushroom"-shaped in three-dimensional form (same as in Fig. 5.2-4), the top of which is shaded with blue lines, at depths of 12-18 km. Below the NE part of this body, Moho depth is not well resolved. Along the coast of the Antarctic Peninsula the Moho depth is about 34 km, and along the South Shetland Islands crustal thickness reaches 35 km. The latter area separates Bransfield Strait from the South Shetland Trench, where the minimum Moho depth in the area occurs (12 km).

Discussion

On the SW end of landward projection of the HFZ we detected two HVB's with *Vp*>7.2 km s^{-1}. The geometry of our network of measurements, for obvious reasons, was not optimal to detect details of the structure of the whole landward projection of HFZ. From our data we can not prove or disprove connection between the HVB's in the south; but we are sure of a their separation from the HVB of Bransfield Strait by a zone of lower velocities. The extend of the HVB in Bransfield Strait is controlled by rifting processes at its NE limit. Can we connect existence of HVBs, expressed on both transects, with the landward extension of HFZ? One explanation could be movements along the boundary between a passive and an active margin (?rotation of South Shetland Microplate), which could create conditions for injection of upper mantle material into the crust, or uplift of the lower crust.

In the NE part of the Bransfield Strait where the larger "mushroom" HVB has its root, velocity increases continuously to 7.8 km s^{-1} at 30 km depth. This suggests the existence of a thick crust-mantle transition zone, often encountered in active rift zones, rather than a step-like Moho boundary. Therefore, the area marked by violet colour on Fig. 5.2-4, indicates that the velocity isolines do not reflect the Moho discontinuity depth.

The papers by Barker et al. (2003) and Christeson et al. (2003) present the results of a wide-angle seismic experiment with a net of eight profiles, conducted in Bransfield Strait in 2000. Christeson et al. (2003) detected, similarly to our investigations, velocities >7.25 km s^{-1} at a depths 10-15 km at the central part of Bransfield Strait, which they interpreted as the Moho boundary. In our interpretation it is the top of HVB (Fig. 5.2-4). The well documented upper mantle velocity Vp>8.0 km s^{-1} on the record sections along 300 km of DSS-20 profile (Grad et al. 1997), strong reflections from the Moho boundary observed on DSS-17 profile (Grad et al. 1993) and lower velocities (~6.9 km s^{-1}) detected below HVB along DSS-3 profile (Janik 1997a,b) confirm our interpretation of the Moho boundary at a depth of ~30 km below Bransfield Strait.

Conclusions

- Maximum crustal thickness of 38-42 km occurs along the Antarctic Peninsula shelf between Adelaide Island and Palmer archipelago.
- Towards the Pacific, the Moho depth decreases and reaches 30-32 km at the edge of study area.
- Minimum Moho depth in the study area is beneath the South Shetland Trench (12 km).
- In the central part of the Bransfield Strait seismic velocities reach an anomalously high value of 7.2 km s^{-1} at 13-18 km depth in the "mushroom"-shaped body.
- In the NE part of Bransfield Strait, near the axis of the active rift, velocities increasing from 7.2 to 7.7 km s^{-1} were found.
- The area of shallow Moho depths (ca. 30 km) in central part of the Bransfield Strait extends between the coast of the Antarctic Peninsula, with a Moho depth about 34 km, and South Shetland Islands, with a Moho depth of 35 km.
- On the landward projection of the HFZ, two high velocity bodies with Vp>7.2 km s^{-1} were detected, both separated from the HVB of the Bransfield Strait by a zone of lower velocities with Vp<6.6 km s^{-1}.

Acknowledgements

The authors are grateful to Prof. G.R. Keller from University of Texas at El Paso and to referee, Dr. R.D. Larter from British Antarctic Survey for their constructive criticism and helpful comments.

References:

Barker PF (1982) The Cenozoic subduction history of the Pacific margin of the Antarctic Peninsula: ridge-crest interactions.- Journal of the Geological Society, London, 139: 787-802

Barker DHN, Christeson GL, Austin JA, Dalziel IWD (2003) Backarc basin evolution and cordilleran orogenesis: Insights from new ocean-bottom seismograph refraction profiling in Bransfield Strait, Antarctica, Geology 31 (2): 107-110

BAS (1985) Tectonic map of the Scotia arc, 1:3000000, Sheet 3. British Antarctic Survey, Cambridge

Birkenmajer K, Gutерch A, Grad M, Janik T, Perchuć E (1990) Lithospheric transect Antarctic Peninsula, South Shetland Islands, West Antarctica. Polish Polar Res 11: 241-258

Cande SC, Kent DV (1995) Revised calibration of the geomagnetic polarity timescale for the Late Cretaceous and Cenozoic, J Geophys Res 100: 6093-6095

Christeson GL, Barker DHN, Austin JA, Dalziel IWD (2003) Deep crustal strusture of Bransfield Strait: initiation of a backarc basin by rift reactivation and propagation, J Geophys Res 108(10):2492

Červený V, Pšenčík I (1983) Program SEIS83, numerical modelling of seismic wave fields in 2-D laterally varving bedded structures by ray method. Charles University, Praha

Eagles G, 2004. Tectonic evolution of the Antarctic Phoenix plate system since 15 Ma. Earth Planet Sci Letters 217: 97-109

Gambôa LAP, Maldonado PR (1990) Geophysical investigation in the Bransffield Strait and Bellingshausen Sea.- Antarctica. In: John BST (ed) Antarctica as an Exploration Frontier. Amer Assoc of Petrol Geol 31, Tulsa, pp 127-141

Garrett SW, Storey BC (1987) Litospheric extension on the Antarctic Peninsula during Cenozoic subduction. In: Coward MP, Dewey JF, Hancock PL (eds) Continental extension tectonics. Geol Soc , London Spec Publ 28: 419-431

Grad M, Gutерch A, Środa P, (1992) Upper crustal structure of Deception Island, the Bransfield Strait, West Antarctica. Antarctic Sci 1: 460-476

Grad M, Gutерch A, Janik T (1993) Seismic structure of the lithosphere across the zone of subducted Drake plate under the Antarctic plate, West Antarctica. Geophys J Internat 115: 586-600

Grad M, Shiobara H, Janik T, Gutерch A, Shimamura H (1997) New seismic crustal model of the Bransfield Rift, West Antarctica from OBS refraction and wide - angle reflection data. Geophys J Internat 130: 506-518

Grad M, Gutерch A; Janik T, Środa P (2002) In: Gamble JA; Skinner DNB; Henrys S (eds) Antarctica at the close of a millennium. Royal Soc New Zealand Bull 35: 493-498

Gutерch A, Grad M, Janik T, Perchuć E, Pajchel J (1985) Seismic studies of the crustal structure in West Antarctica 1979-1980 - preliminary results. Tectonophysics 114: 411-429

Gutерch A, Grad M, Janik T, Perchuć E (1991) Tectonophysical models of the crust between the Antarctic Peninsula and the South Shetland Trench. In: Thomson MRA, Crame JA, Thomson JW (eds) Geological Evolution of Antarctica. Cambridge University Press, Cambridge, pp 499-504

Gutерch A, Grad M, Janik T, Środa P (1998) Polish Geodynamical Expeditions – seismic structure of West Antarctica. Polish Polar Res 19: 113-123

Henriet PJ, Meissner R, Miller H, GRAPE Team (1992) Active margin processes along the Antarctic Peninsula. Tectonophysics 201: 229-253

Herron EM, Tucholke BE (1976) Sea-floor magnetic patterns and basement structure in the souteastern Pacific. In: Hollister CD, Craddock C et al. (eds) Initial Reports of the Deep Sea Drilling Project. U.S. Government Printing Office, Washington DC, pp 263-278

Jabaloy A, Balanyá J-C, Barnolas A, Galindo-Zaldívar J, Hernández J, Maldonado A, Martínez-Martínez J-M, Rodríguez-Fernánez J, de Galdeano CS, Somoza L, Suriñach E, Vásquez JT (2003) The transition from an active to a passive margin (SW and of the South Shetland Trench, Antarctic Peninsula). Tectonophysics 366: 55-81

Janik T (1997a) Seismic crustal structure in the transition zone between Antarctic Peninsula and South Shetland Islands. In: Ricci CA (ed.) The Antarctic Region: geological evolution and processes. Terra Antarctica Publication, Siena, pp 679-684

Janik T (1997b) Seismic crustal structure of the Bransfield Strait, West Antarctica. Polish Polar Res 18: 171-225

Jin YK, Larter RD, Kim Y, Nam Sh, Kim KJ (2002) Post-subduction margin structures along Boyd Strait, Antarctic Peninsula. Tectonophysics 346: 187-200

Komminaho K (1998) Software manual for programs MODEL and XRAYS - a graphical interface for SEIS83 program package. University of Oulu, Dep Geophys, Rep 20, pp 1- 31

Larter RD, Barker PF (1991) Effects of ridge crest-trench interaction on Antarctic-Phoenix spreading: forces on a young subducting plate. J Geophys Res 96(12): 19583-19604

Larter RD, Rebesco M, Vanneste LE, Gambôa LAP, Barker PF (1997) Cenozoic tectonic, sedimentary and glacial history of the continental shelf west of Graham Land, Antarctic Peninsula. In: Barker PF and Cooper AK (eds) Geology and seismic stratigraphy of the Antarctic Margin, 2. Amer Geophys Union Antarc Res Ser 71: 1-27

Livemore RA, Balayá J-C, Maldonado A, Martínez-Martínez J-M, Rodríguez-Fernández J, de Galdeano CS, Galindo-Zaldívar J, Jabaloy A, Somoza L, Hernández J, Molina J, Suriñach E, Viseras C (2000) Autopsy on a dead spreading center: the Phoenix Ridge, Drake Passage, Antarctica. Geology 28: 607-610

Maldonado A, Larter R, Aldaya F (1994) Forearc tectonic evolution of the South Shetland margin, Antarctic Peninsula. Tectonics 1: 1345-1370

Pelayo AM, Wiens DA (1989) Seismotectonics and relative plate motions in the Scotia Sea region. J Geophys Res 94: 7293-7320

Środa P, (1999) Modification to software package ZPLOT by CA Zelt. Inst Geophys Polish Acad Sci

Środa P (2001) Three-dimensional modelling of the crustal structure in the contact zone between Antarctic Peninsula and South Pacific from seismic data. Polish Polar Res 22: 129-146

Środa P (2002) Three-dimensional seismic modelling of the crustal structure between the South Pacific and the Antarctic Peninsula. In: Gamble JA, Skinner DNB, Henrys S (eds) Antarctica at the close of a millennium. Royal Soc New Zealand Bull 35: 555-561

Środa P, Grad M, Guterch A (1997) Seismic models of the Earth's crustal structure between the South Pacific and the Antarctic Peninsula. In: Ricci CA (ed) The Antarctic Region: geological evolution and processes. Terra Antarctica Publication, Siena, pp 685-689

Tomlinson JS, Pudsey CJ, Livermore RA, Larter RD, Barker PF (1992) Long-range side scan sonar (GLORIA) survey of the Pacific margin of the Antarctic Peninsula. In: Yoshuide Y, et al. (eds) Recent progress in Antarctic earth science. Terra Scientific Publishing, Tokyo, pp 423-429

Wessel P, Smith WHF (1995) New version of generic mapping tools released. EOS 76: 329

Zelt CA (1994) Software package ZPLOT, Bullard Laboratories, University of Cambridge